Structure and Dynamic Stereochemistry of Trimesitylmethane. II. Empirical Force Field Calculations[1]

Joseph D. Andose and Kurt Mislow*

Contribution from the Department of Chemistry, Princeton University, Princeton, New Jersey 08540. *Received August 16, 1973*

Abstract: The static and dynamic stereochemistry of trimesitylmethane (**1**) has been investigated utilizing the approach of full relaxation empirical force field calculations. **1** adopts a propeller geometry (C_3) in the ground state. Geometric parameters are indicative of a molecule accommodating some degree of strain due to the presence of the *o*-methyl substituents. Specifically, elongation of the central C–C bond to 1.55 Å and enlargement of the central C–C–C angle to 117.7° was found. The dihedral angle subtended by the plane of a given mesityl ring and a plane containing the C_3 axis and passing through the central bond to that ring is 40.7°. Support for the calculated geometry of **1** derives from a comparison with X-ray structural data for dimesityl-1-(2,4,6-trimethoxyphenyl)methane and trimesitylborane. Calculated activation energies for the idealized one-, two-, and three-ring flip stereoisomerization mechanisms are 47, 31, and 80 kcal/mol, respectively. Calculations were performed which describe in some detail the pathway corresponding to the lowest energy isomerization (*i.e.*, two-ring flip) mechanism. The calculated activation energy of 20 kcal/mol for this process compares favorably with the value (21.9 kcal/mol) found experimentally.

As part of our continuing interest in the complexities of isomerism and isomerization in molecules possessing two or more aryl groups bonded to a central atom,[2] we have undertaken a study of the static and dynamic stereochemistry of trimesitylmethane (**1**), utilizing the approach of full relaxation empirical force field calculations. The present paper describes the results of this study.

In the preceding paper[2h] the dynamic stereochemistry of **1** was explored by the use of nmr spectroscopy. Although that study yielded an energy barrier for the process corresponding to the site exchange of the diastereotopic *o*-methyl protons, it was not possible to arrive at a definitive choice among alternative mechanisms on the basis of the experimental data alone. The present investigation into the stereochemistry of **1** was launched in order to examine in some detail the pathway corresponding to the stereoisomerization process of lowest energy (*threshold mechanism*), and to calculate an activation energy for this process. In the course of attaining these objectives, a force field and methodology was developed that is capable of application to more complex examples of isomerism in aryl compounds, both as an aid to the interpretation of experimental results and as a predictive tool.

Description of Empirical Force Field

The literature contains numerous investigations of various degrees of sophistication which are concerned with the application of the empirical force field approach to the study of the structure of compounds containing aromatic rings.[3-9] As the starting point for the present calculations, we chose to employ the force field of Allinger and coworkers.[10] This force field has been defined for a number of functional groups, and is one of the most thoroughly tested of the force fields currently available.[11] To this force field, we added parameters which permit the treatment of aromatic rings.[12] Additionally, it was found necessary to incorporate special minimization algorithms (see below) required to permit the attainment of the minimum energy conformation. The potential functions comprising our empirical force field are summarized in eq 1, and the force field parameters are collected in Table I.

$$E_{\text{steric}} = \Sigma E_{\text{stretch}} + \Sigma E_{\text{bend}} + \Sigma E_{\text{twist}} + \Sigma E_{\text{nonbonded}} + \Sigma E_{\text{out-of-plane}} + \Sigma E_{\text{stretch-bend}} \quad (1)$$

(1) This work was supported by the National Science Foundation (GP-30257).

(2) (a) D. Gust and K. Mislow, *J. Amer. Chem. Soc.*, **95**, 1535 (1973); (b) J. F. Blount, P. Finocchiaro, D. Gust, and K. Mislow, *ibid.*, **95**, 7019 (1973); (c) P. Finocchiaro, D. Gust, and K. Mislow, *ibid.*, **95**, 7029 (1973); (d) R. J. Boettcher, D. Gust, and K. Mislow, *ibid.*, **95**, 7157 (1973); (e) M. G. Hutchings, C. A. Maryanoff, and K. Mislow, *ibid.*, **95**, 7158 (1973); (f) K. Mislow, D. Gust, P. Finocchiaro, and R. J. Boettcher, *Fortschr. Chem. Forsch.*, 47, 1 (1974); (g) D. Gust, P. Finocchiaro, and K. Mislow, *Proc. Nat. Acad. Sci. U. S.*, 70, 3445 (1973); (h) P. Finocchiaro, D. Gust, and K. Mislow, *J. Amer. Chem. Soc.*, **96**, 2165 (1974); (i) *ibid.*, **96**, 2176 (1974).

(3) N. A. Ahmed, A. I. Kitaigorodsky, and K. V. Mirskaya, *Acta Crystallogr., Sect. B*, 27, 867 (1971); A. I. Kitaigorodsky and V. G. Dashevsky, *Tetrahedron*, **24**, 5917 (1968); *Theor. Exp. Chem. (USSR)*, **3**, 18 (1967); V. G. Dashevsky and A. I. Kitaigorodsky, *ibid.*, **3**, 22 (1967); V. G. Dashevsky, Yu. T. Struchkov, and Z. A. Akopyan, *J. Struct. Chem. (USSR)*, 7, 555 (1966); V. G. Dashevsky, *ibid.*, 7, 83 (1966); **6**, 850 (1965).

(4) T. Beringhell, A. Gavezzotti, and M. Simonetta, *J. Mol. Struct.*, **12**, 333 (1972); G. Casalone and M. Simonetta, *J. Chem. Soc. B*, 1180 (1971); G. Casalone, C. Mariani, A. Mugnoli, and M. Simonetta, *Mol. Phys.*, **15**, 339 (1968); *Theor. Chim. Acta*, **8**, 228 (1967).

(5) (a) R. H. Boyd, S. N. Sanwal, S. Shary-Tehrany, and D. McNally, *J. Phys. Chem.*, **75**, 1264 (1971); (b) S.-J. Chang, D. McNally, S. Shary-Tehrany, M. J. Hickey, and R. H. Boyd, *J. Amer. Chem. Soc.*, **92**, 3109 (1970); (c) C.-F. Shieh, D. McNally, and R. H. Boyd, *Tetrahedron*, **25**, 3653 (1969); (d) R. H. Boyd, *J. Chem. Phys.*, **49**, 2574 (1968).

(6) G. Montaudo and P. Finocchiaro, *J. Mol. Struct.*, **14**, 53 (1972); *J. Amer. Chem. Soc.*, **94**, 6745 (1972); G. Montaudo, P. Finocchiaro, and S. Caccamese, *J. Org. Chem.*, **38**, 170 (1973); G. W. Buchanan, G. Montaudo, and P. Finocchiaro, *Can. J. Chem.*, **51**, 1053 (1973).

(7) (a) N. L. Allinger and M. T. Tribble, *Tetrahedron Lett.*, 3259 (1971); (b) N. L. Allinger and J. T. Sprague, *J. Amer. Chem. Soc.*, **95**, 3893 (1973).

(8) A. Warshel and M. Karplus, *ibid.*, **94**, 5612 (1972).

(9) J. J. Daly, F. Sanz, R. P. A. Sneeden, and H. H. Zeiss, *J. Chem. Soc., Perkin Trans. 2*, 1614 (1972); A. Mannschreck and L. Ernst, *Chem. Ber.*, 104, 228 (1971); T. J. Weismann and J. C. Schug, *J. Chem. Phys.*, **40**, 956 (1964).

(10) (a) N. L. Allinger, M. T. Tribble, M. A. Miller, and D. W. Wertz, *J. Amer. Chem. Soc.*, **93**, 1637 (1971); (b) N. L. Allinger and J. T. Sprague, *ibid.*, **94**, 5734 (1972); (c) N. L. Allinger, M. T. Tribble, and M. A. Miller, *Tetrahedron*, **28**, 1173 (1972); (d) M. T. Tribble and N. L. Allinger, *ibid.*, **28**, 2147 (1972).

(11) For a recent evaluation of empirical force field calculations, as applied to saturated hydrocarbons, see E. M. Engler, J. D. Andose, and P. v. R. Schleyer, *J. Amer. Chem. Soc.*, **95**, 8005 (1973).

(12) The present work was completed prior to the appearance of Allinger's most recent work[7b] dealing with unsaturated systems.

Table I. Empirical Force Field Parameters[a,b]

	Stretch	
	k_r	r^0
H–C_{sp^3}	4.60	1.094
H–C_{ar}	5.05	1.090
C_{sp^3}–C_{sp^3}	4.40	1.512
C_{sp^2}–C_{ar}	4.40	1.500
C_{ar}–C_{ar}	7.65	1.390

	Bend (k_3' = −0.401)		
	NH[c]	k_θ	θ^0
H–C_{sp^3}–H	3	0.20	111.2
	2	0.20	112.8
H–C_{sp^3}–C	3	0.24	107.8
	2	0.24	108.5
	1	0.24	108.4
C–C_{sp^2}–C	2	0.40	110.2
	1	0.40	110.6
	0	0.40	109.5
C_{ar}–C_{ar}–C_{ar}		0.50	120.0
C_{ar}–C_{ar}–C_{sp^3}		0.35	120.0
C_{ar}–C_{ar}–H		0.20	120.0

	Twist			
	V_0	B	n	ϕ_{max}
H–C_{sp^3}–C_{sp^3}–H	0.50	1.0	3	60
H–C_{sp^3}–C_{sp^3}–C	0.50	1.0	3	60
C–C_{sp^3}–C_{sp^3}–C	0.50	1.0	3	60
H–C_{ar}–C_{ar}–H	0.0			
H–C_{ar}–C_{ar}–C	0.0			
C_{sp^3}–C_{ar}–C_{ar}–C	0.0			
C_{ar}–C_{ar}–C_{ar}–C_{ar}	−11.52	−1.0	2	90
C_{ar}–C_{ar}–C_{sp^3}–H	0.014	1.0	6	30
C_{ar}–C_{ar}–C_{sp^3}–C	0.014	1.0	6	30

	Nonbonded[d,e]							
	Parameter set							
	A		B		C		D	
X	$\frac{1}{2}d_{xx}^*$	ϵ_{xx}	$\frac{1}{2}d_{xx}^*$	ϵ_{xx}	$\frac{1}{2}d_{xx}^*$	ϵ_{xx}	$\frac{1}{2}d_{xx}^*$	ϵ_{xx}
H	1.50	0.06	1.50	0.06	1.50	0.06	1.50	0.06
C_{sp^3}	1.50	0.116	1.50	0.116	1.50	0.116	1.50	0.116
C_{ar}	1.85	0.033	2.30	0.01	1.95	0.06	1.85	0.12

	Out-of-plane[f]	
	k_δ	δ^0
(C_{ar}–C_{ar}–C_{ar})–H	0.29	0.0
(C_{ar}–C_{ar}–C_{ar})–C	0.80	0.0

	Stretch-bend
	$k_{r\theta}$
H–C_{sp^3}–H	0.0
H–C_{sp^3}–C	−0.04
C–C_{sp^2}–C	−0.09

[a] Potential functions are given in eq 1. [b] The following units apply: angstroms (r^0 and d^*); degrees (θ^0, δ^0, ϕ_{max}); millidynes angstroms^{-2} (k_r); millidynes radians^{-2} (k_θ, k_δ); millidynes angstroms^{-1} radians^{-1} ($k_{r\theta}$); radians^{-1} (k_3'); kcal/mol (V_0, ϵ). Atom hybridizations, where important, are included as subscripts, *e.g.*, C_{ar} denotes an aromatic-type carbon. [c] Total number of hydrogens bonded to central atom. [d] Nonbonded 1,3 interactions and nonbonded interactions between aromatic carbon atoms in the *same* benzene ring are excluded from consideration. [e] Parameter d (eq 1) refers to the distance between the centers of electron density for a pair of atoms involved in a nonbonded interaction. For all atoms except hydrogen, the center of electron density is taken to coincide with the nuclear position. For a hydrogen atom bonded to X, the center of electron density is arbitrarily displaced from the hydrogen nucleus by 8% of the H–X bond length along the direction of the H → X bond vector (see ref 10a). [f] For the general out-of-plane interaction of the form "(a–b–c)–d," the variable δ (eq 1) represents the angle by which bond vector b–d deviates from the plane defined by atoms a, b, and c.

where

$$E_{stretch} = \tfrac{1}{2}k_r(r - r^0)^2$$

$$E_{bend} = \tfrac{1}{2}k_\theta(\Delta\theta^2 + k_3'\Delta\theta^3);\ \Delta\theta = \theta - \theta^0$$

$$E_{twist} = \tfrac{1}{2}V_0(B + \cos n\phi) \text{ for } |\phi| \leq \phi_{max}$$

$$= 0 \text{ for } |\phi| > \phi_{max}$$

$$E_{nonbonded} = 8.28 \times 10^5\epsilon_{ab}\exp(-d/0.0736d_{ab}^*) - 2.25\epsilon_{ab}(d_{ab}^*/d)^6$$

$$\epsilon_{ab} = \sqrt{\epsilon_{aa}\epsilon_{bb}}$$

$$d_{ab}^* = \tfrac{1}{2}(d_{aa}^* + d_{bb}^*)$$

$$E_{out\text{-}of\text{-}plane} = \tfrac{1}{2}k_\delta(\delta - \delta^0)^2$$

$$E_{stretch\text{-}bend} = k_{r\theta}(|r_{ab} - r_{ab}^0| + |r_{bc} - r_{bc}^0|)(|\Delta\theta_{abc}|)$$

Treatment of Aromatic Rings. We have adopted, in general, Boyd's[5] treatment of the strain components in aromatic rings, employing those of his parameters for stretching, bending, and twisting that apply to aromatic rings, but we have scaled his bending parameters to conform with similar parameters in the Allinger force field.[10] As initial parameters for the aromatic carbon nonbonded function, we used the values given by Allinger[10b] for olefinic carbon. This trial set of nonbonded parameters is denoted as set A (Table I).

Calculations[13] were performed with parameter set A on a number of molecules (*i.e.*, 2,2-paracyclophane (**2**), Table II; 2,2-metacyclophane (**3**), Table III; triphenylmethane (**4**), Table IV; and phenylcyclohexane (**5**), Table V) for which structure or energy data are available. Such calculations should, therefore, serve as tests of the reliability of our parameter set for aromatic rings. For the purpose of comparison, results for the same set of molecules employing the Boyd force field[5a,b] are included in Tables II–V.

The results of these calculations for **2** (Table II, set A) and **3** (Table III, set A) revealed a deficiency in our choice of nonbonded parameters for aromatic carbon. Thus, the separation of carbons in opposing rings is approximately 0.25 Å smaller than experimental. Consequently, we treated the parameters for the aromatic carbon nonbonded potential as adjustable, and generated three new sets of parameters (Table I, sets B–D) which reproduce the inter-ring separation d(2- - -8) in **2** (Table II).[14]

Using parameter sets B–D, calculations were repeated for the remaining molecules (**3**–**5**) of our test series and the results are summarized in Tables III–V. We note that the structures thus calculated are very nearly identical; even the phenyl twist angle in **4** is insensitive to our choice of nonbonded potential as represented by parameter sets B–D. Only in the case of the calculations for **5**, and, to a lesser extent, for **3**, can some preference among these parameter sets be found. Thus,

(13) Calculations were carried out on an IBM 360/91 computer using double precision arithmetic. Analysis was aided by viewing all structures in three dimensions using the facilities of the Princeton Computer Graphics Laboratory (E & S LDS-1/DEC PDP-10), supported in part by a grant from the National Institutes of Health.

(14) Two parameters, d^* and ϵ, are required to set the nonbonded potential for aromatic carbon in the Hill[15] formulation of the nonbonded potential (see eq 1). In deriving just three parameter sets of the many possible, we have chosen three values of ϵ which span the anticipated range for this parameter, and for each value of ϵ so chosen have determined a corresponding value of d^*.

(15) T. L. Hill, *J. Chem. Phys.*, **16**, 399 (1948).

Table II. 2,2-Paracyclophane (**2**)

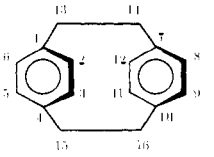

	Exptl[a,b]	Boyd force field[c]	Present force field[d] parameter set[e] A	B	C	D
r(1,13)	1.540 (1.547)	1.516	1.520	1.531	1.529	1.529
r(13,14)	1.548 (1.630)	1.563	1.553	1.564	1.563	1.563
$r(C_{ar}-C_{ar})$	1.39–1.40	Av 1.392	Av 1.393	Av 1.395	Av 1.394	Av 1.393
θ(1,2,3)	120.2 (119.1)	119.7	120.2	120.4	120.3	120.3
θ(1,13,14)	114.6 (111.2)	112.4	109.9	113.2	113.4	113.5
θ(2,1,6)	118.6 (119.7)	119.1	118.4	117.5	117.7	117.8
θ(2,1,13)	119.9 (119.9)	119.8	120.4	120.7	120.5	120.5
d(1- - -7)	2.83 (2.751)	2.721	2.585	2.770	2.780	2.783
d(2- - -8)	3.09 (3.087)	3.019	2.845	3.089	3.095	3.093

[a] Unparenthesized values by C. J. Brown, *J. Chem. Soc.*, 3265 (1953). [b] Parenthesized values by K. Lonsdale, H. J. Milledge, and K. V. Krishna Rao, *Proc. Roy. Soc., Ser. A*, **255**, 82 (1960). [c] Our calculations employing the Boyd force field of ref 5a and 5b. [d] See Table I. [e] Nonbonded parameter sets; see Table I.

Table III. 2,2-Metacyclophane (**3**)

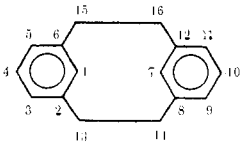

	Exptl[a]	Boyd force field[b]	Present force field[c] parameter set[d] A	B	C	D
r(6,15)	Av 1.534	1.515	1.520	1.531	1.529	1.529
r(15,16)	1.559	1.557	1.545	1.557	1.555	1.555
$r(C_{ar}-C_{ar})$	Av 1.386	Av 1.391	Av 1.393	Av 1.394	Av 1.394	Av 1.393
θ(1,6,5)	117.3	119.1	118.4	117.7	117.8	117.8
θ(1,6,15)	120.2	118.6	118.6	118.5	118.3	118.4
θ(2,1,6)	122.3	120.4	121.5	122.1	121.9	121.8
θ(6,15,16)	110.3	111.8	111.2	113.3	113.3	113.2
d(1- - -7)	2.689	2.581	2.503	2.666	2.698	2.716

[a] C. J. Brown, *J. Chem. Soc.*, 3278 (1953). [b] See footnote *c* in Table II. [c] See footnote *d* in Table II. [d] See footnote *e* in Table II.

Table IV. Triphenylmethane (**4**)

	Exptl[a]	Boyd force field[b]	Present force field[c] parameter set[d] A	B	C	D
$r(C_{sp^3}-C_{ar})$	1.53	1.517	1.520	1.538	1.534	1.533
$r(C_{ar}-C_{ar})$	1.40	Av 1.391	Av 1.393	Av 1.399	Av 1.394	Av 1.393
$\theta(C_{ar}-C_{sp^3}-H)$		106.8	105.0	103.5	103.9	104.0
$\theta(C_{ar}-C_{sp^3}-C_{ar})$	112 ± 2	112.1	113.6	114.8	114.4	114.4
$\phi(H-C_{sp^3}-C_{ar}-C_{ar})$	45 ± 5	34.4	40.5	35.0	35.7	36.2

[a] P. Andersen, *Acta Chem. Scand.*, **19**, 622 (1965). [b] See footnote *c* in Table II. [c] See footnote *d* in Table II. [d] See footnote *e* in Table II.

Table V. Phenylcyclohexane: Conformational Energy (*A* Value) of a Phenyl Substituent in the Cyclohexane Series

	Exptl	Boyd force field[b]	Present force field[c] parameter set[d] A	B	C	D
A value	3.0[a]	3.4	3.4	3.2	2.8	2.4

[a] Average of several values, reported in "Table of Conformational Energies," by J. A. Hirsch, *Top. Stereochem.*, **1**, 199 (1967). [b] See footnote *c* in Table II. [c] See footnote *d* in Table II. [d] See footnote *e* in Table II.

parameter sets B and C give a better value than parameter set D for d(1- - -7) in **3**. Similarly, parameter sets B and C bracket the experimental *A* value for a phenyl substituent in the cyclohexane series. Parameter set C was adopted in preference to set B for all subsequent calculations since it employs a value of ϵ (eq 1) that does not lie at either extreme of the anticipated range for this parameter.

The present scheme ignores effects due to the conjugation of adjacent p–π centers.[16] This is not expected to pose a serious limitation, however, since direct conjugation of an aromatic ring with a substituent is not possible for the compounds discussed in this paper.

Minimization Methods. The varieties of energy minimization techniques and their relative advantages and disadvantages have been discussed.[17] For the

(16) Force fields which include separate treatment of the σ and the π framework have been reported.[4,7b,8]

(17) J. E. Williams, P. J. Stang, and P. v. R. Schleyer, *Annu. Rev. Phys. Chem.*, **19**, 531 (1968).

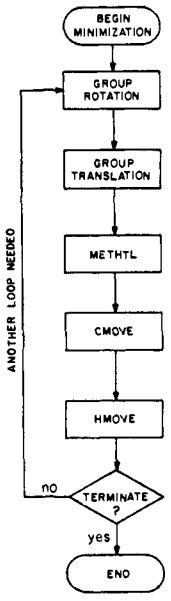

Figure 1. Flow diagram for the energy minimization module.

present study, we have experimented with the "steepest descent," "pattern search," and "parabolic prediction" methods, the latter based on a quadratic expansion of the potential surface.

In our hands, we experienced the greatest success with the pattern search minimization technique as implemented by Williams, Stang, and Schleyer.[17] Difficulties were encountered, however, for calculations on molecules that incorporate aromatic rings. Thus, none of the above methods were successful in rotating aromatic rings significantly from their initial input positions. As a result, utilization of several different input geometries for the same molecule resulted in "minimized" structures which were significantly different. This behavior is not surprising, since rotation of an aryl ring requires the concerted motion of the atoms composing the aromatic ring, while most minimization methods involve the motion of only a single atom (or a single carbon and attached hydrogens) at a time.

In order to remedy this situation, we prefixed our pattern minimization routines CMOVE[18] and HMOVE[18] with special subroutines which rotate and translate aryl groups as rigid units to a position of minimum energy. Also included ahead of CMOVE and HMOVE was a subroutine to rotate methyl groups to a position of minimum energy. A flow diagram of our minimization module is given in Figure 1. The minimization loop is terminated when the energy decrease relative to the preceding loop falls below 0.01 kcal/mol.

Ground State Structure of Trimesitylmethane

The structure of **1** in the ground state has been calculated by full relaxation empirical force field calculations using the method and force field described above. Results of this calculation are summarized in Figure 2a

(18) In routine CMOVE, all non-hydrogen atoms are moved, one at a time, to positions of minimum energy. During this process, attached hydrogen atoms are carried along in a rigid translation.[19] In routine HMOVE, non-hydrogen atoms are not treated while all hydrogen atoms are individually permitted to seek their minimum energy position. Routines CMOVE and HMOVE have been adapted from the strain program of Williams, Stang, and Schleyer.[17]

(19) As suggested by K. B. Wiberg, *J. Amer. Chem. Soc.*, 87, 1070 (1965).

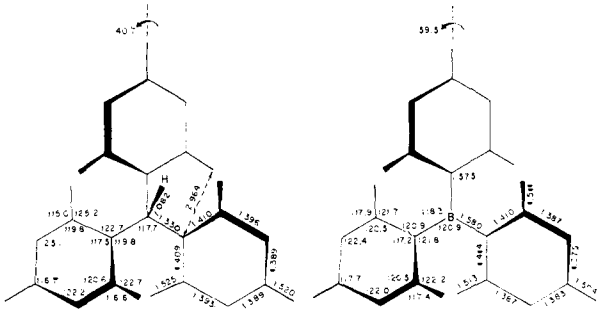

Figure 2. (a) Calculated ground-state structure of trimesitylmethane (**1**) (left). (b) X-Ray structural data for trimesitylborane (**7**) (right); see ref 2b.

and a stereoscopic view of the calculated structure, including hydrogens, is provided in Figure 3.

The calculation indicates that **1** adopts a propeller conformation (C_3) in the ground state, and in that respect corresponds to other molecules possessing three aromatic rings bonded to a central atom.[20] Nmr data for **1** are consistent with this conformation in solution.[2h]

Geometric parameters in **1** are indicative of a molecule accommodating a considerable amount of strain, due to the presence of bulky *o*-methyl substituents. This may be appreciated most readily by a comparison of our calculated structure for triphenylmethane (**4**, Figure 4) with that calculated for **1** (Figure 2a). Thus, bond lengths to the central carbon are 1.55 Å in **1**, as compared with 1.53 Å in **4** (1.53 Å experimental, see Table IV) and 1.505 Å for an average C_{sp^3}–C_{sp^2} (aromatic) bond.[21] Similarly, the central bond angle in **1**, 117.7°, is more than three degrees greater than that in **4** (114.3° calculated, 112 ± 2° experimental; see Table IV). Another indication of the strain present in **1** is found in the distribution of angles α and β to the central carbon. At each of the α positions, there are two C–C–C angles external to the aromatic ring, one proximal and the other distal to the methine hydrogen. In **4**, these two angles are nearly equal, but in **1** the distal angle (122.7°) exceeds the proximal (119.8°) by *ca.* 3°. At the β position, steric accommodation is indicated by the opening of the C–C–Me angle (125.2°), reflecting the need to maximize the separation of the distal methyl from the adjacent aromatic ring. The distortion is almost entirely in-plane; distortion of the C–Me bonds from the plane of the appropriate aromatic ring does not exceed 1.3°. Even with these distortions at the α and β positions, however, a distal methyl carbon atom approaches to within 2.964 Å of a carbon atom on the adjacent aromatic ring (Figure 2a). This distance is significantly less than the distance parameter for this interaction (d^* = 3.45 Å; see Table I).

While the structure of **1** has not as yet been determined experimentally, the details of our calculation receive strong support from an X-ray structural determination of dimesityl-1-(2,4,6-trimethoxyphenyl)-methane (**6**).[22] Specifically, the Mes–C–Mes angle (Mes = mesityl) for **6**, reported[22] as 117.8°, compares well with our calculated value of 117.7° for **1**. Similarly, the angles α to the central carbon in **6** follow a similar trend to that calculated for **1** (proximal, 117.4 (**6**)

(20) See footnotes 4 and 5 in ref 2a.

(21) L. E. Sutton, Ed., *Chem. Soc., Spec. Publ.*, No. 18, S 21s (1965).

(22) M. J. Sabacky, S. M. Johnson, J. C. Martin, and I. C. Paul, *J. Amer. Chem. Soc.*, 91, 7542 (1969).

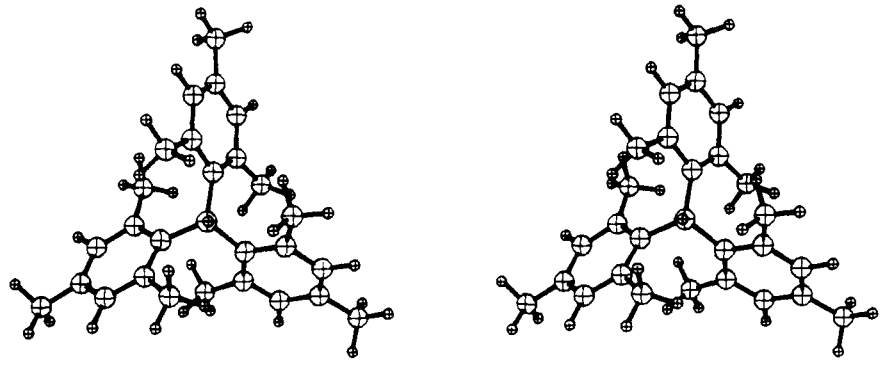

Figure 3. Stereoscopic view of the calculated ground-state structure of **1**.

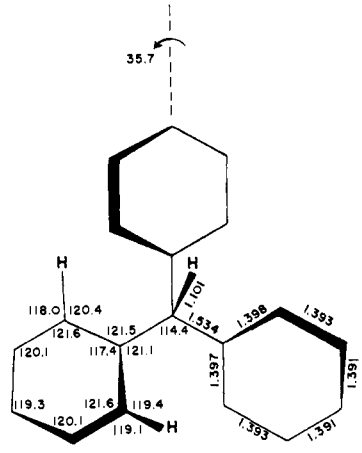

Figure 4. Calculated ground-state structure of triphenylmethane (**4**).

and 119.8 (**1**); distal, 125.7 (**6**) and 122.7 (**1**)). Finally, the distance between the distal methyl carbon atom for one mesityl ring and the closest carbon of the adjacent mesityl ring is 2.966 Å in **6** and 2.964 Å in **1**.

Additional support for our calculated structure derives from a comparison of the X-ray structure[2b] for trimesitylborane (**7**, Figure 2b) with that calculated for **1** (Figure 2a). This comparison is made viable by the happenstance that steric interactions in **1** create a central geometry similar to that in **7**. Detailed examination of Figures 2a and 2b reveals a remarkable similarity in structure for these two molecules. Thus, bond lengths and bond angles in the mesityl rings for each molecule are very nearly the same, any deviations being well within the error limits of the experimental determination. Finally, the dihedral angles (ϕ) formed by the planes of the mesityl rings with respect to appropriate planes of reference[23] are 39.3° for **7** and 40.7° for **1**.

Dynamic Stereochemistry of Trimesitylmethane and Cognate Systems

The ambient temperature (37°) ^{1}H-nmr spectrum (60 MHz) of **1** in hexachloro-1,3-butadiene solution[2h] displays three resonances of equal intensity in the methyl region, an observation, as noted above, consistent with our calculated ground-state structure. When the sample of **1** is warmed, the two upfield methyl signals (assigned to the diastereotopic *o*-methyl protons) broaden and ultimately coalesce at 167°.[2h] Application of the Gutowsky–Holm approximation[24] yielded a rate constant of 37.7 sec^{-1} at 167°, corresponding to the exchange in environment of the *o*-methyl protons for all three mesityl groups.

Stereoisomerization in molecules of this type (Ar_3ZX) has been commonly interpreted in terms of five possible mechanisms:[2a] inversion along the central Z–X bond, plus four rotational mechanisms which have been denoted[25] as the zero-, one-, two-, and three-ring flip mechanisms.[26] In the case of **1**, the observed dnmr process was discussed in terms of the aforementioned mechanisms.[2h] The inversion mechanism was rejected since it requires the breaking of the central C–H bond, and the zero-ring flip mechanism was ruled out on simple steric grounds. The data, however, did not permit a choice between the one- and the two-ring flip mechanisms. Furthermore, although the three-ring flip mechanism cannot explain the nmr results, the experimental data provided no information concerning the rate of this process.

Discrimination among the Flip Mechanisms. We have performed calculations designed to assess the energies of the idealized transition states for the one-, two-, and three-ring flip mechanisms.[26] Although the activation energies obtained in this manner are necessarily crude estimates for the actual barriers, the results have qualitative, if not semiquantitative significance in ranking the various rotational mechanisms for the stereoisomerization (*i.e.*, enantiomerization) of **1**.

The input structures for these calculations differed solely in the orientation of the mesityl rings about the central C–Mes bonds, *i.e.*, in the value of ϕ as dictated by the particular flip mechanism under consideration. All input structures shared the following common features. The central carbon was positioned at the origin and the methine hydrogen was placed on the *z* axis. The mesityl rings were placed about the central carbon in such a way that bond lengths to the central carbon were initially 1.50 Å and bond angles to the central carbon were all tetrahedral. The mesityl rings themselves were regular planar hexagons with a C–C bond length of 1.39 Å.

During minimization, the following degrees of freedom and constraints were imposed. The central carbon

(23) Defined in this context as the plane(s) containing the C_3 axis and one of the bonds to the central atom.

(24) H. S. Gutowsky and C. H. Holm, *J. Chem. Phys.*, **25**, 1288 (1956).

(25) The flip mechanisms were first postulated by Kurland, *et al.*, in discussing triarylcarbenium ions: R. J. Kurland, I. I. Schuster, and A. K. Colter, *J. Amer. Chem. Soc.*, 87, 2279 (1965).

(26) See Figure 2 in ref 2a. All of these mechanisms necessarily result in a reversal of helicity.

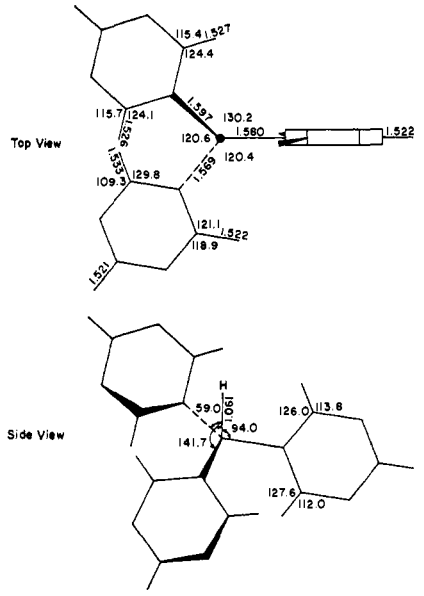

Figure 5. Calculated structure of the idealized one-ring flip transition state for **1**. The heavy dot indicates a hydrogen pointing toward the observer.

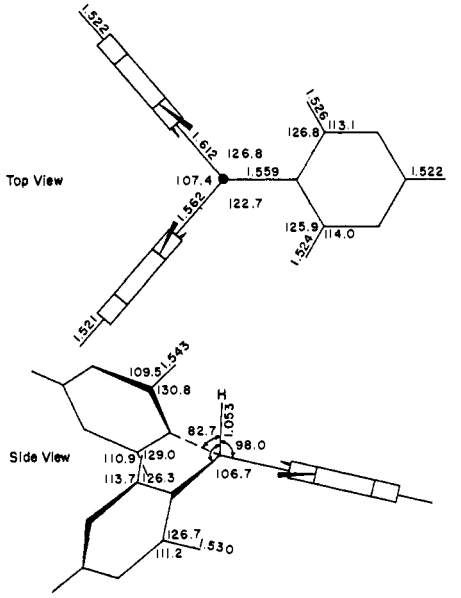

Figure 6. Calculated structure of the idealized two-ring flip transition state for **1**.

atom was frozen at the origin and the methine hydrogen was free to move only along the z axis. Carbon atoms of the mesityl ring were not permitted individual and independent movement, since this would have destroyed the desired orientation (twist angle) of the ring about the C–Mes bond. Consequently, the rings were constrained to retain the geometry of a plane regular hexagon throughout. Atoms comprising the methyl groups and all hydrogens of the mesityl rings were permitted full freedom of movement. Movement of the mesityl rings was accomplished by replacement of the subroutines for group rotation and group translation (Figure 1) with a special subroutine which moves individual mesityl rings as rigid units in spherical coordinate space. Relaxation of the C–Mes (C = central carbon atom) bonds and the H–C–Mes and the Mes–C–Mes bond angles was thereby accomplished, without changing the input H–C–C_{ar}–C_{ar} dihedral angles, ϕ.

Results of these calculations are summarized in Figures 5–7 for the idealized one-, two-, and three-ring flip transition states, respectively. Large geometric distortions were found for all three transition-state models, a direct result of the circumstance that each possesses an energy significantly (30–80 kcal/mol) above that of the ground state. Each idealized transition state model was input with the highest symmetry allowed for that particular form (C_s for the one- and two-ring flips and C_{3v} for the three-ring flip). However, due to the staggering of adjacent mesityl rings resulting from unfavorable nonbonded interactions, all resulting structures became asymmetric (C_1).

Calculated activation energies for the one-, two-, and three-ring flip stereoisomerization mechanisms, based upon the idealized transition states, are 47, 31, and 80 kcal/mol, respectively. The two-ring flip mechanism is assessed as the lowest energy pathway for isomerization, with the one-ring flip and the three-ring flip representing higher energy processes.

These calculations have quantitative significance only to the extent that the idealized transition states (Figures 5–7) are representative of the actual transition states for

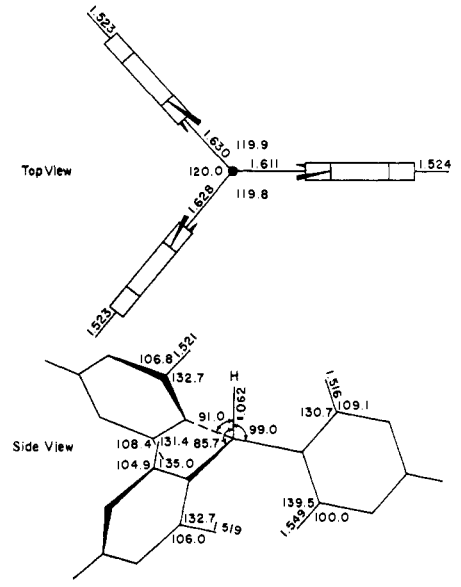

Figure 7. Calculated structure of the idealized three-ring flip transition state for **1**.

the processes under investigation. In the following section, we shall examine in more detail the pathway corresponding to the lowest activation energy.

The Stereoisomerization Pathway. Calculations were performed designed to examine in detail the pathway corresponding to the actual stereoisomerization of **1**. Our starting point was the ground-state structure of **1**, as calculated in the previous section, in one of its enantiomeric forms (Figure 8). From this starting point, two independent series of calculations were generated. In the first of these, series A, one mesityl ring was rotated about its C–Mes bond by 10° increments in a counterclockwise sense,[27] thereby generating new struc-

(27) By "clockwise" and "counterclockwise" we mean the direction of motion as seen from the central carbon atom, looking toward the mesityl ring. In series A and B, the reference structure (ground state), arbitrarily taken as the enantiomer depicted in Figure 8, might be thought of as the Δ form by analogy with the stereochemically correspondent[2b,f] Δ-tris-tridentate transition metal complexes.

Table VI. Calculation of the Stereoisomerization Pathway for Trimesitylmethane[a]

Series A					Series B				
Calcn no.	ϕ_1	ϕ_2	ϕ_3	Steric energy	Calcn no.	ϕ_1	ϕ_2	ϕ_3	Steric energy
1	140.0	138.3	138.9	25.4	1	140.0	138.3	138.9	25.4
2	130.0	142.8	140.6	25.8	14	150.0	133.4	136.8	26.2
3	120.0	149.3	140.9	27.4	15	160.0	130.6	133.2	28.6
4	110.0	156.1	141.7	30.6	16	170.0	131.7	123.4	31.3
5	100.0	163.8	143.7	34.9	17	180.0	133.5	116.4	34.3
6	90.0	171.8	146.8	39.7	18	−170.0	133.8	110.5	36.8
7	80.0	−177.3	150.4	44.6	19	−160.0	135.2	104.5	40.6
12	75.0	−172.2	153.8	46.7	20	−150.0	138.9	97.6	45.8
8	70.0	−167.2	157.7	49.5	23	−145.0	142.8	93.3	47.9
13	65.0	−154.7	173.0	47.0	21	−140.0	155.4	84.7	48.4
9	60.0	−148.3	−176.1	40.8	24	−135.0	−176.6	66.8	35.4
10	50.0	−136.0	−147.9	28.5	22	−130.0	−175.3	65.0	34.1
11	40.0	−133.9	−141.0	26.4					
7a	80.0	−175.5	152.0	43.4	20a	−150.0	136.4	97.3	43.3
12a	75.0	−169.5	157.5	45.0	23a	−145.0	141.9	92.4	45.7
8a	70.0	−144.3	−165.3	33.4	21a	−140.0	−150.0	54.9	27.4

[a] Steric energy in kcal/mol; ϕ_1, ϕ_2, and ϕ_3 in degrees (refer to Figure 8 and text).

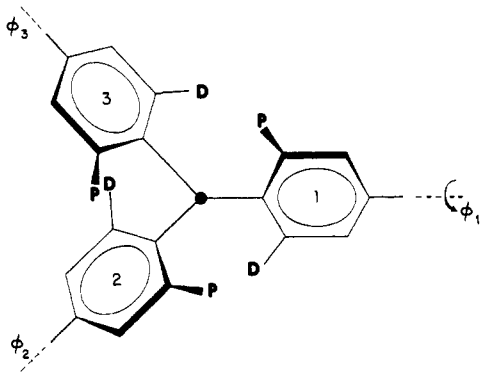

Figure 8. Initial conformation for the calculations (Table VI) of the stereoisomerization pathway for **1**. The dihedral angle ϕ_1 refers to the orientation of the ring being driven, in this case, in a clockwise[27] direction (series B). Distal and proximal methyl groups for the structure shown are identified as D and P, respectively.

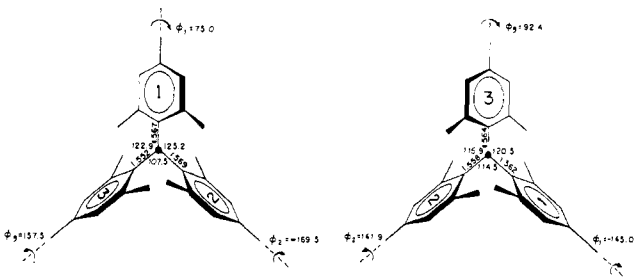

Figure 9. Approximate transition-state structures for the stereoisomerization of **1**: (a) structure corresponding to calculation number 12a, series A, in Table VI (left); (b) structure corresponding to calculation number 23a, series B, in Table VI (right).

tures for each incremental change. At each stage, the structure was subjected to a full relaxation empirical force field calculation, with the exception that the dihedral angle ϕ formed by the incremented mesityl ring and the reference plane[23] was held constant during energy minimization. The second series of calculations, series B, differs from the first only in the direction (*i.e.*, clockwise) of rotation about the C–Mes bond.[27]

The results of these calculations, two series of structures and their corresponding steric energies, are collected in Table VI. In this table, individual calculations are numbered, number 1 corresponding to the ground-state structure (Figure 8). The identifiers ϕ_1, ϕ_2, and ϕ_3 refer to the central H–C–C_{ar}–C_{ar} dihedral angle[28] for the three correspondingly numbered mesityl rings in Figure 8.

Initial calculations in each series (calculations 1–11 and 14–22) were performed allocating a limited amount of computer time (5 min) for each calculation. These preliminary calculations served to locate, approximately, the transition state for isomerization in each series. Additional interpolative calculations (12–13 and 23–24) in the neighborhood of the highest energy structures, using a smaller (5°) rotational increment, permitted a closer approach to the transition-state geometry and energy. Given the limited time allocation, the geometries and steric energies listed do not correspond to full minimization. Nevertheless, geometric parameters are very close to final values,[29] at least for structures leading up to the transition state.[30]

Calculations were followed to completion in the neighborhood of the transition state in order to permit estimation of an activation energy for each process (calculations 7a, 8a, 12a, 20a, 21a, and 23a).[31]

As revealed by comparison of the data in Table VI, series A, as mesityl ring 1 is driven from its initial orientation by a succession of incremental rotations in the counterclockwise direction (ϕ_1, 140° → 40°), both remaining mesityl rings describe rotations in the opposite (clockwise)[27,28] direction. Examination of the orientations of the mesityl rings from start (calculation 1) to finish (calculation 11) shows that we have effected an enantiomerization of **1**. Thus, the twist angle of each ring has been reversed, thereby reversing the pitch (helicity) of the molecular propeller.

(28) The angles are defined as positive for a clockwise rotation[27] of a given mesityl ring with respect to its reference plane,[23] taking as $\phi = 0°$ that position in which the distal methyl group (D in Figure 8) is cis to the methine hydrogen.

(29) In the final stages of minimization the steric energy decreases very slowly and during this time the geometric parameters change very little.

(30) Once past the transition state, energy and geometry change drastically.

(31) Comparison of entries for calculations 7 and 7a, 12 and 12a, 20 and 20a, and 23 and 23a supports our contention that geometric parameters found in the preliminary series, for calculations leading to the transition state, are very close to final values.

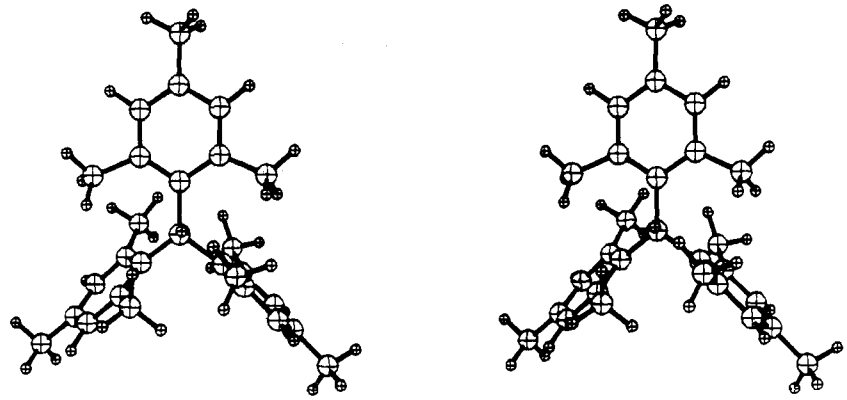

Figure 10. Stereoscopic view corresponding to the structure shown in Figure 9a.

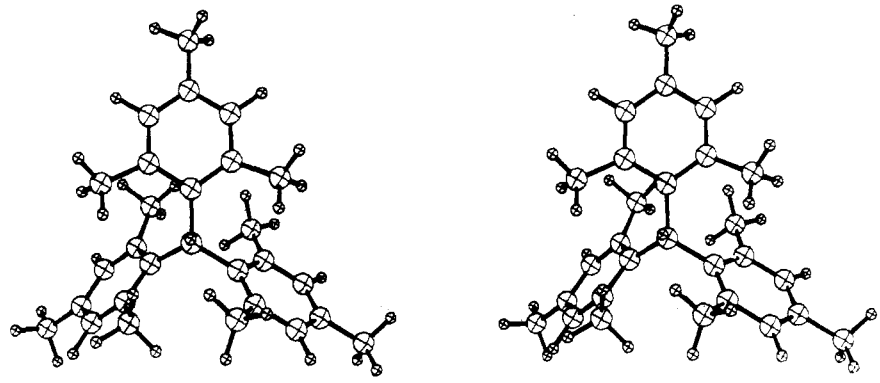

Figure 11. Stereoscopic view corresponding to the structure shown in Figure 9b.

Similarly, in series B, as mesityl ring 1 is driven from its initial orientation by a succession of incremental rotations in the clockwise direction (ϕ_1, $140° \rightarrow -140°$), one of the remaining mesityl rings (ring 2) describes a net rotation in the same direction, while the other one (ring 3) moves in the opposite direction. Once again, as seen by comparison of the orientation of the mesityl rings from start (calculation 1) to finish (calculation 21a), enantiomerization of **1** has been effected.

The transition states for the stereoisomerization depicted in series A and B occur somewhere in the vicinity of the structures calculated in 12a and 23a, respectively (Table VI). Taking the steric energy of 12a and 23a as representative of the transition state, the activation energy is calculated to be 19.6 and 20.3 kcal/mol, respectively.

Structural details for calculations 12a and 23a—calculations closest to the transition states for series A and B, respectively— are summarized in Figures 9a and 9b. Corresponding stereoscopic views are shown in Figures 10 and 11. The geometries of 9a and 9b differ in detail, but both can be derived from Figure 6 by a slight relaxation of the constraints imposed by the idealized two-ring flip model.

Indeed, it must be stated at this juncture that the differences calculated for the stereoisomerization pathways in series A and series B are undoubtedly an artifact of our somewhat coarse approach. In series A, the unique, nonflipping ring is driven, while the other rings follow. In series B, on the other hand, it is one of the flipping rings which is driven, while the other two follow. Thus, the two series in effect focus on different portions of the molecule in the course of the same two-ring flip isomerization process, *i.e.*, they depict different aspects of the same phenomenon. The transition-state geometries and energies should therefore in principle be the same. It follows that the actual transition state lies somewhere near 9a or 9b, and the activation energy approximates 20 kcal/mol, in excellent agreement with the value of 21.9 kcal/mol experimentally found for the exchange of *o*-methyl protons.[2h] Consequently, this exchange process is identified by the present calculations as the two-ring flip mechanism.[32]

The agreement between calculated and experimental values may be taken as an index both of the quality of our force field and of the quality of our description of the stereoisomerization process.

Our conclusion that the two-ring flip is the threshold mechanism for the enantiomerization of **1** is consistent with results for related systems. The enantiomerization of trimesitylsilane[2d] and related silanes,[2d] as well as the stereoisomerization of triarylcarbenium ions,[2a,33] has been discussed in terms of the two-ring flip mechanism. Further, providing the absence of accidental isochrony or fortuitously equivalent rates for competing processes, the coalescence of the *o*-methyl group resonances in the ^{1}H-nmr spectrum of **6**[22] is consistent only with the two-ring flip mechanism,[2a] or with a permutationally analogous process which does not include a change of helicity. Granted the same assumptions,

(32) In series A and in series B, the identities of proximal and distal methyl groups are exchanged for one mesityl ring (ring 1 in series A and ring 3 in series B) and retained for the two remaining rings. This is precisely the net stereochemical result expected for the two-ring flip mechanism.

(33) J. W. Rakshys, Jr., S. V. McKinley, and H. H. Freedman, *J. Amer. Chem. Soc.*, **93**, 6522 (1971).

identical conclusions follow from studies of other triarylmethyl systems,[2f] triarylboranes,[2b] and triarylamines.[3,4]

Acknowledgment. We are indebted to Professors Paul v. R. Schleyer and W. Todd Wipke for access to strain programs developed in their respective research groups which aided in the formulation of our own computer program. We would also like to thank Princeton University for a generous allotment of computer time.

(34) D. Hellwinkel, M. Melan, and C. R. Degel, *Tetrahedron*, 29, 1895 (1973).

Stereochemistry of Dimesityl-9-anthrylmethane and Bis(2,6-xylyl)-1-(2-methylnaphthyl)methane. Evidence for the Two-Ring Flip Mechanism in Triarylmethanes[1]

Paolo Finocchiaro,[2] Devens Gust, and Kurt Mislow*

Contribution from the Department of Chemistry, Princeton University, Princeton, New Jersey 08540. *Received August 16, 1973*

Abstract: The temperature-dependent ^{1}H-nmr spectra of the title compounds indicate that these molecules adopt a propeller conformation in the ground state, and that a variety of interconversions of stereoisomeric molecules on the nmr time scale occurs at elevated temperatures. These interconversions are all shown to proceed by the two-ring flip mechanism. The associated free energies of activation are reported. Comparison of the present results with the results of earlier studies on triarylmethanes, triarylboranes, and cognates brings to light that the two-ring flip mechanism is the favored stereoisomerization pathway for all of these systems.

The previous papers in this series[3] discussed the stereochemistry of trimesitylmethane (**1**), which represents the simplest stereochemical class of triarylmethanes in that all three aryl groups are the same and possess local C_2 axes. Since the degeneracies inherent in this system do not permit the assignment of a stereoisomerization mechanism solely on the basis of nmr spectroscopic evidence, ancillary arguments were needed.

The present report deals with stereoisomerism and stereoisomerization in two triarylmethane systems of greater complexity, dimesityl-9-anthrylmethane (**2**) and bis(2,6-xylyl)-1-(2-methylnaphthyl)methane (**3**). The analysis of stereoisomerization for these two systems is somewhat more involved than that for **1**, but by the same token yields more mechanistic information, and allows assignment of stereoisomerization mechanisms on nmr spectroscopic evidence alone. In addition, this study allows a comparison between the stereochemistry of **2** and **3** and that of their boron analogs, whose properties have been reported earlier.[4]

Dimesityl-9-anthrylmethane (2). By analogy with **1** and related compounds,[3] **2** and **3** are both presumed to adopt the propeller conformation in the ground state. The sense of twist of the propeller may be either right- or left-handed, and **2** therefore exists in two enantiomeric forms, similar to the case of **1**.[3] However, one of the degeneracies present in **1** (a C_3 molecule) has been removed by replacing one mesityl group by a 9-anthryl group. Thus **2** is asymmetric (even though all three rings possess local C_2 axes and two of the rings are the same), and all four of the *o*-methyl groups of each enantiomer are diastereotopic, as are the two *p*-methyl groups. In the absence of accidental isochrony, the ^{1}H-nmr spectrum of **2** in an achiral medium should therefore feature four signals for the *o*-methyl groups and two for the *p*-methyl groups.

At 23° the 60-MHz ^{1}H-nmr spectrum of a $CHBr_3$ solution of **2** displays five methyl resonances in a ratio of intensities of *ca.* 2:1:1:1:1 (Figure 1). The four upfield resonances are due to the four diastereotopic *o*-methyl groups, which are shielded by the aromatic rings. The more intense downfield resonance is due to the two diastereotopic *p*-methyl groups, which are accidentally isochronous. The low-temperature spectrum is thus in accord with the postulated propeller conformation.

The possible stereoisomerization pathways for **2** may be divided into five classes: inversion along the C–H bond, and four classes of flip mechanisms.[3,5] As in the case of **1**, each enantiomer of **2** has available one inversion, one zero-ring flip, and one three-ring flip pathway. However, in contrast to **1**, since the molecule no longer has C_3 symmetry the system is now capable of undergoing three discrete two-ring flips and three discrete one-ring flips.

These pathways are shown graphically in Figure 2. The two vertices represent the enantiomers of **2**, and the edges represent stereoisomerizations. The edges are

(1) This work was supported by the National Science Foundation (GP-30257).

(2) NATO Fellow, 1972–1973, on leave of absence from the University of Catania, Catania, Italy.

(3) (a) P. Finocchiaro, D. Gust, and K. Mislow, *J. Amer. Chem. Soc.*, 96, 2165 (1974); (b) J. D. Andose and K. Mislow, *ibid.*, 96, 2168 (1974).

(4) J. F. Blount, P. Finocchiaro, D. Gust, and K. Mislow, *J. Amer. Chem. Soc.*, 95, 7019 (1973).

(5) (a) D. Gust and K. Mislow, *J. Amer. Chem. Soc.*, 95, 1535 (1973). (b) The flip rearrangements result both in permutations of ligand positions and in a change of helicity of the molecular propeller. Another set of rearrangements which do not involve a net change of helicity is conceivable. All the available evidence[3] suggests that the flip pathways are of lowest energy, and consequently we have limited our discussion to that set.